in the absorption intensity in the region of 480 nm for the arthropods.[61]

On the basis of the UV-vis properties, model-building studies, and initial observations concerning the reactivity of these $Cu_2(NnPY2)(O_2)]^{2+}$ complexes,[62] we currently favor either a nonplanar structural type *a* or *c* for the coordinated peroxo group in $Cu_2(N4PY2)(O_2)]^{2+}$ (**3**). EXAFS spectroscopic studies on **3** and the other $[Cu_2(NnPY2)(O_2)]^{2+}$ complexes are in progress,[47] and these may be useful in distinguishing between structural possibilities.

Summary

We have presented evidence that, at low temperatures, the reaction of dioxygen with the dicopper(I) complex, $[Cu_2(N4PY2)]^{2+}$ (**2**), results in the formation of a dioxygen/copper adduct, $[Cu_2(N4PY2)(O_2)]^{2+}$ (**3**), which is best described as a peroxo-dicopper(II) species. The binding of O_2 is reversible (Figure 1), and cycling experiments can be carried out such that O_2 can be removed from **3** by the application of a vacuum, resulting in the regeneration of **2** and the recovery of dioxygen. In addition, carbon monoxide can be used to displace dioxygen from **3**, such that when CO is reacted with $[Cu_2(N4PY2)(O_2)]^{2+}$ (**3**), O_2 is liberated, and the dicarbonyl adduct, $[Cu_2(N4PY2)(CO)_2]^{2+}$ (**1**), is formed. The carbon monoxide ligands in **1** can then be removed at room temperature under a partial vacuum, with the regeneration of **2**; subsequent cooling and addition of O_2 result in the reformation of the dioxygen adduct, **3**. No oxidation product (e.g. CO_2 or carbonates or oxidized N4PY2 product) has been observed in these reactions.

The electronic absorption spectrum of the dioxygen complex **3** and the other $[Cu_2(NnPY2)(O_2)]^{2+}$ species bear a close resemblance to that observed for oxyhemocyanins. The most striking aspect of these synthetic efforts involving $Cu-O_2$ reactivity using NnPY2 ligands is the ability to produce a system with the multiple and exceedingly strong CT bands, particularly the near-UV band (360 nm (ϵ 14 000–19 000 M^{-1} cm^{-1}) for **3**, Table VI; 345 nm (ϵ 20 000 M^{-1} cm^{-1}) for oxy-Hc). The presence of a strong band (ϵ 3500–5500 M^{-1} cm^{-1}) in the 400–500-nm region for $[Cu_2(NnPY2)(O_2)]^{2+}$ may possibly be explained by a distortion from planarity of the $Cu(II)_2-(O_2^{2-})$ unit in these synthetic systems, a necessity which is also borne out by an examination of molecular models of possible structures of $[Cu_2(N4PY2)(O_2)]^{2+}$ (**3**).

Thus, we have been able to mimic to a significant extent a number of properties of hemocyanins, including the reversible binding of CO and O_2 and the major features of the UV-vis spectroscopy. Current efforts include further structural and spectroscopic characterization of the dioxygen complexes, examination of their reactivity, and systematic modification of the NnPY2 ligands.

Acknowledgment. We thank the National Institutes of Health for their generous support of this research. We also acknowledge Professor E. I. Solomon and J. E. Pate of Stanford University and Dr. N. J. Blackburn of UMIST, England, for helpful discussions. We also thank Brett Cohen for help in obtaining NMR spectra.

Registry No. **1**-$(PF_6)_2$, 98218-45-2; **1**-$(ClO_4)_2$, 112022-76-1; **1a**-$(PF_6)_2$, 112022-70-5; **1a**-$(ClO_4)_2$, 112022-71-6; **1a**-$(BF_4)_2$, 112022-77-2; **2**-$(PF_6)_2$, 112022-72-7; **2**-$(ClO_4)_2$, 112022-73-8; **3**, 112022-74-9; **4**, 112022-75-0; N4Py2, 98218-51-0; $[Cu(CH_3CN)_4](PF_6)$, 64443-05-6; 1,4-diaminobutane, 110-60-1; 2-vinylpyridine, 100-69-6.

Supplementary Material Available: Listings of bond lengths, bond angles, anisotropic temperature factors, and hydrogen coordinates and temperature factors for complexes **1a**-$(ClO_4)_2$ (Tables VIII–XI) and **2**-$(ClO_4)_2$ (Tables XIII–XVI) (8 pages); listings of observed and calculated structure factors for **1a**-$(ClO_4)_2$ (Table VII) and **2**-$(ClO_4)_2$ (Table XII) (16 pages). Ordering information is given on any current masthead page.

(61) Himmelwright, R. S.; Eickman, N. C.; LuBien, C. D.; Solomon, E. I. *J. Am. Chem. Soc.* **1980**, *102*, 5378–5388.

(62) Preliminary indications are that these dioxygen complexes are relatively unreactive, and thus we think that the O_2 is very tightly bound (e.g. possibly mode *c*). An example of this is the observation that at −80 °C *no* reaction (as followed spectroscopically) occurs upon the addition of 2 equiv of a strong acid (e.g. HPF_6) to $[Cu_2(N4PY2)(O_2)]^{2+}$ (**3**). Thus, the coordinated O_2^{2-} moiety in **3** is not basic; this is in contrast to the corresponding result obtained with $[Cu_2(XYL\text{-}O\text{-})(O_2)]^{+}$ (**B**), where protonation readily produces a hydroperoxo complex, $[Cu_2(XYL\text{-}O\text{-})(O_2H)]^{+}$.[19]

A Deoxymyoglobin Model with a Sterically Unhindered Axial Imidazole

Michel Momenteau,*[1] W. Robert Scheidt,*[2] C. W. Eigenbrot,[2] and Christopher A. Reed*[3]

Contribution from the Institut Curie, Section de Biologie, Centre Universitaire, 91405 Orsay, France, the Department of Chemistry, University of Notre Dame, Notre Dame, Indiana 46556, and the Department of Chemistry, University of Southern California, Los Angeles, California 90089-1062. *Received June 8, 1987*

Abstract: With use of an $\alpha,\alpha,\alpha,\alpha$-tetra-*o*-amido functionalized tetraphenylporphyrin having *trans*-dipivalamido pickets and a *trans*-NH–C(O)–$(CH_2)_6$–C(O)–NH– strap, a single-face hindered porphyrin is produced. Its iron(II) complex attains only five-coordination with the unhindered axial ligand 1-methylimidazole. The product has been isolated as a toluene solvate and characterized by magnetic susceptibility (μ_{eff}^{300K} = 5.4 μ_B), Mossbauer spectroscopy (ΔE_q = 2.3 mm/s, δ = 0.88 mm/s at 4.2 K), and single-crystal X-ray structure analysis as a five-coordinate high-spin iron(II) complex. Crystal data: $FeO_4N_{10}C_{66}H_{64}\cdot C_7H_8$, monoclinic, space group $P2_1$, cell constants a = 13.075 (2) Å, b = 17.821 (3) Å, c = 13.862 (2) Å, and β = 89.97 (1)°, Z = 2, 2388 unique observed data (average of two forms), all measurements at 292 K. The complex has an average $Fe-N_p$ bond distance of 2.075 Å, an axial Fe–N distance of 2.134 Å, and an iron(II) displacement of 0.34 Å from the mean plane of the 24-atom core. The structure is compared to other five-coordinate imidazole-ligated metalloporphyrin species reported in the literature. Of greatest interest is the comparison with previously characterized five-coordinate 2-methylimidazole-ligated iron(II) complexes where the 2-methyl substituent on imidazole is the means used to attain five-coordination. A smaller iron atom displacement and less imidazole tilting result from the absence of a 2-methyl group, and these results support the idea of a constrained proximal histidine in T-state deoxyhemoglobin.

Five-coordination in deoxymyoglobin and deoxyhemoglobin is a textbook example of protein control of axial ligation in hemoproteins. Of the several histidine residues in the polypeptide chain only one, the so-called proximal histidine,[4] coordinates to the

0002-7863/88/1510-1207$01.50/0

iron(II) atom despite a strong driving force toward six-coordination. This driving force has been quantified by measuring the successive binding constants for axial ligands coordinating to four-coordinate iron(II) porphyrinates (FeP):[5]

$$FeP + L \underset{}{\overset{K_1}{\rightleftharpoons}} FePL + L \overset{K_2}{\rightleftharpoons} FePL_2$$

For typical nitrogenous bases such as pyridine or imidazole, K_2 is larger than K_1 by a factor of 10 or more. This can be largely understood in terms of the ligand field stabilization energy for the $(t_{2g})^6$ low-spin six-coordinate species. For all practical purposes, five-coordination is unattainable under these conditions. Five-coordination was first achieved by the use of 2-methylimidazole[6] (2-MeHIm); the steric interaction of its methyl group with porphyrin core atoms greatly diminishes K_2 without significantly affecting K_1.[7] This is possible because the five-coordinate species is high spin and its large out-of-plane iron atom displacement allows coordination of a single 2-methylimidazole without severe steric hindrance. The X-ray crystal structure of the high-spin five-coordinate iron(II) tetraphenylporphyrin (TPP) derivative [Fe(TPP)(2-MeHIm)]·C_2H_5OH[8] showed it to be an excellent structural model for deoxymyoglobin. Nonetheless, the question arises as to how much the 2-methyl group influences the coordination parameters. A tilting of the imidazole away from the heme normal, a lengthening of the Fe–N(Im) bond, and the possibility of encouraging porphinato core ruffling are all potential responses of the five-coordinate heme derivative to the presence of the 2-methyl substituent. It would thus be useful to define the coordination geometry intrinsic to a relaxed and unconstrained five-coordinate high-spin iron(II) porphyrinate.

Although the 2-methylimidazole paradigm remains a popular solution to the problem of achieving five-coordination, synthetically elegant tailed, capped, strapped, and pocketed porphyrins[9] have provided a variety of alternate solutions. Many of these methods are superior in that they provide for the use of sterically unhindered imidazoles although some are constrained by tethers of varying potential influence on the coordination group structure. To our knowledge, none of these systems has yielded to a single-crystal structure determination of a deoxymyoglobin model. Hence, it has not been possible to compare hindered and unhindered imidazole-ligated complexes within the meager repertory of isolated deoxyhemoglobin models. Only two structures have been reported;[8,10] both have a 2-methyl substituent on the axial imidazole. In this report, we use a ligand that draws on the concepts of "basket-handle" and "picket fence" porphyrins for controlling axial coordination to produce a porphyrin ligand with one highly hindered face. This "hybrid" porphyrin (Piv_2C_8)[11] is illustrated in the following drawing of our target molecule, a deoxymyoglobin model with an unhindered axial imidazole:

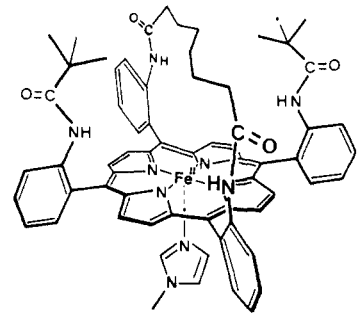

We have successfully isolated this five-coordinate species; we herein report its preparation, magnetic susceptibility, Mössbauer spectrum, and single-crystal structure determination.

Experimental Section

The iron(III) complex [Fe(Piv_2C_8)Cl] was synthesized as previously described.[12] In an inert atmosphere glovebox (O_2 < 1 ppm), [Fe(Piv_2C_8)Cl] (7.3 mg, 0.006 mmol) and 1-methylimidazole (2 mg, 0.024 mmol) in toluene were stirred with amalgamated zinc pellets. Over a 30-min period the brown-green solution turned red-purple (λ_{max} 439 Soret, 540, 561, 607 nm). After filtration through a fine porosity frit, the solution was set aside. Heptane vapor was allowed to diffuse into the solution, and after several days, crystals were harvested, washed with heptane, and mounted in N_2-filled glass capillaries for X-ray diffraction studies. A bulk microcrystalline sample with ~25% ^{57}Fe enrichment was prepared in a similar manner for magnetic and Mössbauer studies.

Magnetic susceptibility data were collected on a SHE Model 905 SQUID susceptometer operating at 10 kG. An 8.3-mg sample, rendered immobile and anaerobic by suspension in a melted, pre-calibrated drop of paraffin wax in an aluminum bucket within the glovebox, was used for the measurement. A diamagnetic correction of 1012×10^{-6} cgs units was used in all calculations.

Mössbauer spectra were taken on the identical sample used for the susceptibility measurements by Ben Shaevitz and Prof. George Lang at The Pennsylvania State University.

A brown needle crystal of [Fe(Piv_2C_8)(1-MeIm)] with approximate dimensions of 0.16 × 0.18 × 0.51 mm was mounted in an N_2-filled glass capillary. All measurements were performed with graphite-monochromated Mo Kα radiation on an Enraf-Nonius CAD4 diffractometer. Preliminary examination suggested a two-molecule monoclinic unit cell. Final cell constants, a = 13.075 (2) Å, b = 17.821 (3) Å, c = 13.862 (2) Å, and β = 89.97 (1)°, came from a least-squares refinement of the setting angles of 25 reflections in the range 20° < $|2\theta|$ < 30°. The calculated cell volume is 3230.1 (19) Å^3. For Z = 2 and a formula of $FeO_4N_{10}C_{66}H_{64}\cdot C_7H_8$, the calculated density is 1.24 g/cm^3 and the observed density was 1.28 g/cm^3. The full-width ω-scan of several intense reflections was 0.32°, indicative of moderate crystal quality. The systematic absences were consistent with the noncentrosymmetric space group $P2_1$ (no 4) or centrosymmetric $P2_1/m$; the noncentrosymmetric assignment was confirmed by all subsequent developments during structure determination and refinement.

Intensity data were measured by the θ–2θ scan method with a constant scan rate of 2° (in θ). Data were collected to a maximum 2θ of 50.0° and standard CAD4 moving-crystal moving-counter background measurements were used for backgrounds (total background counting time $^1/_2$ peak counting time). A total of 11 705 $\pm h$, k, $\pm l$ reflections were measured (5861 unique) along with four standard reflections measured every 60 min during the course of data collection. Intensity data were corrected for absorption during the course of structure refinement (vide infra).

(1) Institut Curie.
(2) University of Notre Dame.
(3) University of Southern California.
(4) Perutz, M. F. *Annu. Rev. Biochem.* **1979**, *48*, 327–386.
(5) Brault, D.; Rougee, M. *Biochemistry* **1974**, *13*, 4591–4597.
(6) Collman, J. P.; Reed, C. A. *J. Am. Chem. Soc.* **1973**, *95*, 2048–2049.
(7) Brault, D.; Rougee, M. *Biochem. Biophys. Res. Commun.* **1974**, *57*, 654–659. Wagner, G. C.; Kassner, R. J. *Biochim. Biophys. Acta* **1975**, *392*, 319–327.
(8) Hoard, J. L. In *Porphyrins and Metalloporphyrins*; Smith, K. M., Ed.; Elsevier: Amsterdam, **1985**; p 317.
(9) Traylor, T. G. *Acc. Chem. Res.* **1981**, *14*, 102–109. Collman, J. P. *Ibid.* **1977**, *10*, 265–272. Baldwin, J. E.; Permutter, P. *Top. Curr. Chem.* **1984**, *121*, 181–220. Momenteau, M. *Pure. Appl. Chem.* **1986**, *58*, 1493–1502. Battersby, A. R.; Hamilton, A. D. *J. Chem. Soc., Chem. Commun.* **1980**. *117*–119. Ward, B.; Chang, C. K. *J. Am. Chem. Soc.* **1981**, *103*, 5236–5241. Eshima, K.; Yuasa, M.; Nishide, H. Tsuchida, E. T. *J. Chem. Soc., Chem. Commun.* **1985**, 130–132. Collman, J. P.; Brauman, J. I.; Collins, T. J.; Iverson, B. L.; Lang, G.; Pettman, R. B.; Sessler, J. L.; Walters, M. A. *J. Am. Chem. Soc.* **1983**, *105*, 3038–3052.
(10) Jameson, G. B.; Molinaro, F. S.; Ibers, J. A.; Collman, J. P.; Brauman, J. I.; Rose, E.; Suslick, K. S. *J. Am. Chem. Soc.* **1980**, *102*, 3224–3237.
(11) Abbreviations used: Piv_2C_8, dianion of α,α,5,15-[2,2′-(octanediamido)diphenyl]-α,α,10,20-bis(o-pivalamidophenyl)porphyrin; TPP-C_3Py, dianion of 5-[2-[(2-(3-pyridyl)ethyl)carbonylamino]phenyl]-10,15,20-triphenylporphyrin; TPP-C_5Im, dianion of *meso*-mono[*o*-(5-(*N*-imidazolyl)valeramido)phenyl]triphenylporphyrin; TPivP, dianion of picket fence porphyrin; TPP, TMPyP, OEP, Proto IX, dianions of *meso*-tetraphenylporphyrin, *meso*-tetra-*N*-methylpyridylporphyrin, octaethylporphyrin, and protoporphyrin IX, respectively; 1-MeIm, 1-methylimidazole; 2-MeHIm, 2-methylimidazole; 1,2-DiMeIm, 1,2-dimethylimidazole; BzIm, benzimidazole; Im$^-$, imidazolate anion; 4-MeIm$^-$, 4-methylimidazolate anion; THT, tetrahydrothiophene.
(12) Momenteau, M.; Loock, B.; Tetreau, C.; Lavalette, D.; Croisy, A.; Schaeffer, C.; Huel, C.; Lhoste, J.-M. *J. Chem. Soc., Perkin Trans. 2* **1987**, 249–257.

Table I. Fractional Coordinates and Thermal Parameters (Å^2) for [Fe(Piv$_2$C$_8$)(1-MeIm)][a]

atom	x	y	z	B(iso)	atom	x	y	z	B(iso)
Fe	0.48564 (20)	0.0000	0.71817 (20)	3.16*	C(7)	0.2858 (13)	−0.0270 (11)	0.4157 (14)	2.9 (4)
N(1)	0.6354 (11)	−0.0254 (9)	0.7467 (10)	3.2 (4)	C(8)	0.2520 (17)	−0.0966 (15)	0.3964 (16)	4.5 (5)
N(2)	0.5203 (10)	−0.0051 (13)	0.5708 (10)	3.7 (3)	C(9)	0.1911 (18)	−0.1093 (16)	0.3184 (18)	6.1 (6)
N(3)	0.3313 (10)	−0.0110 (11)	0.6837 (10)	3.7 (4)	C(10)	0.1745 (19)	−0.0492 (19)	0.2520 (18)	6.2 (7)
N(4)	0.4531 (11)	−0.0283 (9)	0.8598 (10)	3.2 (4)	C(11)	0.2124 (20)	0.0087 (22)	0.2698 (18)	7.0 (6)
C(a1)	0.6768 (16)	−0.0415 (13)	0.8387 (15)	4.5 (5)	C(12)	0.2676 (16)	0.0313 (13)	0.3473 (15)	4.4 (5)
C(a2)	0.7143 (14)	−0.0183 (12)	0.6839 (14)	3.6 (5)	C(13)	0.1651 (15)	0.0002 (20)	0.9107 (14)	4.8 (5)
C(a3)	0.6158 (13)	0.0018 (17)	0.5349 (12)	3.3 (4)	C(14)	0.0936 (16)	−0.0540 (14)	0.9198 (14)	3.9 (5)
C(a4)	0.4490 (14)	−0.0084 (17)	0.4974 (14)	4.7 (5)	C(15)	0.0100 (20)	−0.0469 (17)	0.9863 (19)	6.2 (6)
C(a5)	0.2918 (13)	−0.0092 (15)	0.5949 (12)	3.6 (4)	C(16)	0.0094 (18)	0.0231 (17)	1.0318 (17)	6.4 (7)
C(a6)	0.2524 (14)	−0.0071 (17)	0.7487 (14)	4.3 (5)	C(17)	0.0789 (21)	0.0819 (17)	1.0201 (19)	7.1 (7)
C(a7)	0.3531 (16)	−0.0242 (12)	0.9013 (15)	4.3 (5)	C(18)	0.1628 (21)	0.0665 (19)	0.9558 (19)	7.4 (7)
C(a8)	0.5188 (18)	−0.0384 (14)	0.9331 (16)	5.3 (6)	C(19)	0.6849 (16)	−0.0649 (16)	1.0119 (16)	4.5 (5)
C(b1)	0.7846 (16)	−0.0394 (13)	0.8301 (15)	4.3 (5)	C(20)	0.7312 (20)	−0.1318 (19)	1.0210 (19)	6.9 (7)
C(b2)	0.8067 (16)	−0.0308 (13)	0.7335 (16)	4.4 (5)	C(21)	0.7962 (20)	−0.1438 (17)	1.1141 (20)	7.0 (7)
C(b3)	0.6049 (15)	0.0026 (19)	0.4272 (13)	4.8 (4)	C(22)	0.7962 (18)	−0.0875 (18)	1.1739 (17)	5.6 (6)
C(b4)	0.5039 (13)	−0.0079 (15)	0.4018 (12)	3.7 (4)	C(23)	0.7494 (17)	−0.0250 (15)	1.1687 (16)	5.2 (6)
C(b5)	0.1837 (14)	−0.0051 (18)	0.6029 (13)	4.6 (5)	C(24)	0.6904 (16)	−0.0114 (17)	1.0831 (16)	5.6 (6)
C(b6)	0.1598 (13)	0.0000 (17)	0.6968 (12)	3.7 (4)	C(25)	0.8325 (23)	−0.1863 (20)	0.4299 (21)	7.8 (7)
C(b7)	0.3602 (18)	−0.0327 (13)	0.9984 (16)	5.3 (6)	C(26)	0.7553 (27)	−0.2467 (21)	0.4351 (24)	9.3 (9)
C(b8)	0.4635 (18)	−0.0449 (15)	1.0246 (16)	5.6 (6)	C(27)	0.7820 (31)	−0.2863 (29)	0.5276 (32)	15.1 (15)
C(m1)	0.7061 (13)	−0.0071 (15)	0.5827 (12)	3.2 (4)	C(28)	0.7867 (32)	−0.2992 (26)	0.3368 (29)	14.8 (14)
C(m2)	0.3472 (13)	−0.0151 (13)	0.5077 (12)	3.3 (4)	C(29)	0.6432 (31)	−0.2239 (25)	0.4077 (29)	13.2 (12)
C(m3)	0.2633 (15)	−0.0088 (16)	0.8456 (14)	4.6 (5)	C(30)	0.2739 (27)	−0.2268 (24)	0.4614 (27)	8.9 (9)
C(m4)	0.6243 (14)	−0.0524 (13)	0.9242 (14)	3.4 (4)	C(31)	0.3244 (22)	−0.2673 (18)	0.5403 (20)	7.3 (7)
O(1)	0.9028 (18)	−0.1803 (15)	0.3767 (17)	11.9 (7)	C(32)	0.4000 (22)	−0.2316 (18)	0.6024 (21)	7.8 (8)
O(2)	0.2429 (20)	−0.2611 (18)	0.3884 (20)	14.0 (8)	C(33)	0.4478 (23)	−0.2855 (20)	0.6827 (20)	8.5 (8)
O(3)	−0.0437 (13)	−0.1793 (11)	0.9016 (12)	6.7 (4)	C(34)	0.5264 (21)	−0.2507 (18)	0.7431 (20)	7.0 (8)
O(4)	0.5706 (15)	−0.2111 (11)	0.9634 (12)	8.0 (5)	C(35)	0.5661 (22)	−0.3168 (18)	0.8070 (19)	7.3 (7)
N(5)	0.8041 (15)	−0.1159 (13)	0.4743 (13)	6.0 (5)	C(36)	0.6730 (27)	−0.2843 (23)	0.8604 (25)	11.1 (10)
N(6)	0.2749 (16)	−0.1524 (16)	0.4654 (16)	7.1 (6)	C(37)	0.0309 (19)	−0.1829 (17)	0.8502 (19)	6.1 (6)
N(7)	0.0975 (14)	−0.1159 (13)	0.8635 (13)	5.5 (5)	C(38)	0.0522 (20)	−0.2289 (17)	0.7709 (19)	6.2 (6)
N(8)	0.7341 (16)	−0.1844 (15)	0.9549 (15)	6.4 (5)	C(39)	0.0683 (25)	−0.1939 (22)	0.6818 (25)	10.9 (10)
N(9)	0.4870 (14)	0.1176 (12)	0.7475 (13)	5.2 (5)	C(40)	0.1544 (51)	−0.2681 (42)	0.7960 (42)	23.2 (22)
N(10)	0.5247 (22)	0.2318 (18)	0.7709 (20)	6.5 (7)	C(41)	−0.0317 (32)	−0.2812 (27)	0.7674 (25)	13.6 (13)
C(1)	0.8017 (13)	0.0071 (18)	0.5307 (12)	3.7 (4)	C(42)	0.6590 (25)	−0.2279 (19)	0.9406 (20)	7.7 (8)
C(2)	0.8479 (16)	−0.0489 (14)	0.4725 (14)	3.6 (5)	C(43)	0.5510 (28)	0.1688 (25)	0.7092 (25)	10.8 (10)
C(3)	0.9386 (18)	−0.0353 (15)	0.4223 (17)	4.7 (6)	C(44)	0.4471 (27)	0.2119 (25)	0.8290 (24)	10.2 (10)
C(4)	0.9739 (19)	0.0350 (17)	0.4275 (18)	5.7 (7)	C(45)	0.4376 (25)	0.1435 (23)	0.8175 (24)	8.8 (9)
C(5)	0.9387 (17)	0.0918 (16)	0.4761 (16)	5.6 (6)	C(46)	0.5887 (29)	0.3029 (31)	0.7603 (32)	17.5 (17)
C(6)	0.8434 (17)	0.0789 (15)	0.5312 (15)	4.6 (5)					

[a] The estimated standard deviations of the least significant digit(s) are given in parentheses. The starred atom was treated anisotropically and the isotropic equivalent $B = [V^2 \det(\beta_{ij})]^{1/3}$ is given.

The structure was solved by direct methods using two distinct, complementary approaches. A total of 27 atoms were located from the first E-map calculated with the direct methods program MULTAN78.[13] This emerging model placed the porphyrin core perpendicular to the *y* axis and thus retained the possible mirror symmetry of the space group $P2_1/m$. It should be noted that this mirror would be inconsistent with an ordered structure of [Fe(Piv$_2$C$_8$)(1-MeIm)] and further that the statistics of MULTAN78 indicate an acentric structure. Use of the difference direct methods program DIRDIF[14] produced a reasonable 48-atom model that included some atoms violating the pseudomirror symmetry. Succeeding difference Fourier calculations located remaining atoms. The data were then corrected for the effects of absorption ($\mu = 0.287$ mm^{-1}) with the empirical program DIFABS. After averaging (agreement factors were 4.8% on intensity and 3.7% on F_o), there were 2388 unique data having *I* greater than $2.0\sigma(I)$. These data were used in the final refinement cycles. The toluene molecule of solvation was described as a rigid group. A number of hydrogen atoms were located in difference Fourier syntheses and were included as fixed contributors in subsequent least-squares cycles. Eventually all hydrogen atoms except those of the methyl groups were incorporated into the model and included in the refinement as fixed contributors. Owing to the limited number of data, only the iron(II) atom was refined with anisotropic temperature factors. The final model included 336 variables; the final cycle of full-matrix least-squares had a largest parameter shift of 0.14 times its esd. Final values of the discrepancy indices were 10.46% for the unweighted *R* and 10.78% for the weighted residual.[15] The opposite enantiomer refined to a weighted *R* of 10.84%. The first assignment is thus the correct one at the 0.995 confidence level. A final difference Fourier map was judged to be significantly free of features with the largest peak having a height of 0.60 e/Å^3 and was 1.1 Å from one of the toluene carbon atoms. Final atomic

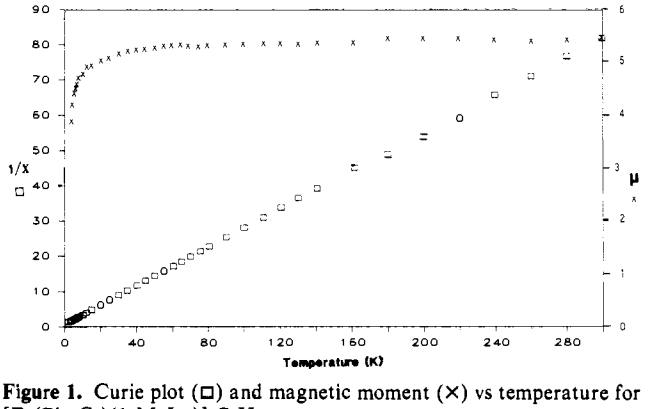

Figure 1. Curie plot (□) and magnetic moment (×) vs temperature for [Fe(Piv$_2$C$_8$)(1-MeIm)]·C$_7$H$_8$.

(13) Programs used in this study included local modifications of Main, Hull, Lessinger, Germain, Declerq, and Woolfson's MULTAN78, Jacobson's ALLS, Zalkin's FORDAP, Busing and Levy's ORFFE and ORFLS, Walker and Stuart's DIFABS, Keller's SCHAKAL and Johnson's ORTEP2. Atomic form factors were from: Cromer, D. T.; Mann, J. B. *Acta Crystallogr., Sect. A* **1968**, *A24*, 321–323. Real and imaginary corrections for anomalous dispersion in the form factor of the iron atom were from: Cromer, D. T.; Liberman, D. J. *J. Chem. Phys.* **1970**, *53*, 1891–1898. Scattering factors for hydrogen were from: Stewart, R. F.; Davidson, E. R.; Simpson, W. T. *Ibid.* **1965**, *42*, 3175–3187. All calculations were performed on a VAX 11/730.

(14) Beurskens, P. T.; Bosman, W. P.; Doesburg, H. M.; Gould, R. O.; van den Hark, Th. E. M.; Prick, P. A. J.; Noordik, J. H.; Beurskens, G.; Parthasarathi, V. DIRDIF Technical Manual 1981/82, Crystallography Laboratory, Toernooivield, Nijmegen, Netherlands.

(15) $R_1 = \sum||F_o| - |F_c||/\sum|F_o|$ and $R_2 = [\sum w(|F_o| - |F_c|)^2/\sum w(F_o)^2]^{1/2}$.

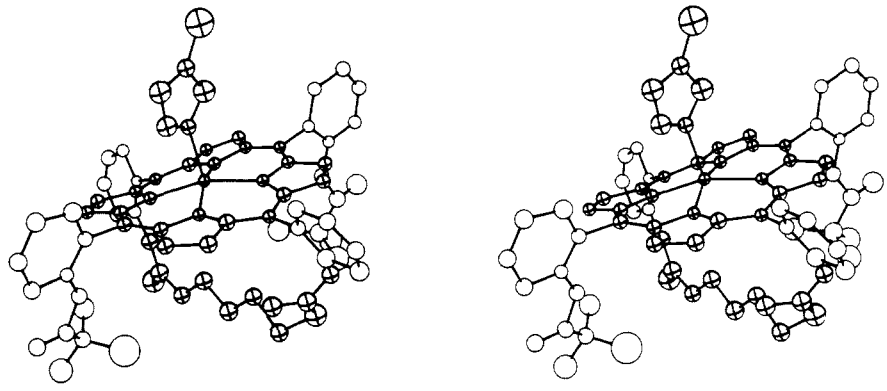

Figure 2. Computer-produced stereoscopic drawing of the [Fe(Piv$_2$C$_8$)(1-MeIm)] molecule in the crystal. Principal and boundary ellipses are drawn for core, strap, and axial ligands; only boundary ellipses are shown for the phenyl and picket atoms. All ellipsoids are contoured at the 50% probability level.

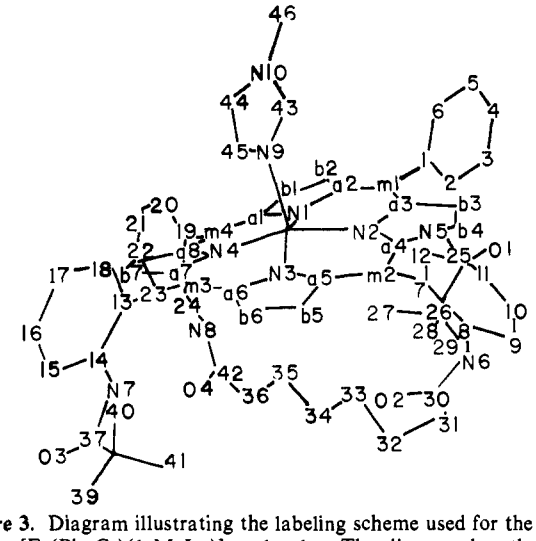

Figure 3. Diagram illustrating the labeling scheme used for the atoms in the [Fe(Piv$_2$C$_8$)(1-MeIm)] molecule. The diagram has the same general orientation as that in Figure 2. Each atom position has been replaced by a label. If no atom symbol is given the atom is a carbon; all other atoms are labeled in the form of an atom symbol followed by a numeric identifier.

coordinates are listed in Table I. The anisotropic thermal parameter for the iron atom, the rigid group parameters for the toluene molecule, the derived atomic coordinates, and the fixed hydrogen atom coordinates are available as supplementary material.

Results and Discussion

The characterization of [Fe(Piv$_2$C$_8$)(1-MeIm)]·C$_7$H$_8$ as a five-coodinate high-spin iron(II) porphyrinate is based upon UV–vis, magnetic susceptibility, Mössbauer, and X-ray crystal data. The electronic spectroscopy has been discussed previously.[12] The magnetic susceptibility data are consistent with an $S = 2$ state. The Curie plot (Figure 1) shows good linearity. The magnetic moment (Figure 1) is essentially constant at about 5.4 μ_B over the temperature range 100–300 K. This is somewhat above the spin-only value of 4.9 but is not outside the range of reported values for high-spin iron(II) (e.g., [Fe(TPP)(THF)$_2$], 5.5 μ_B).[16] The rapid fall-off below 50 K is an expected result of zero-field splitting. The Mössbauer spectrum at 4.2 K in zero applied field shows a quadrupole doublet with $\delta = 0.88$ mm/s relative to metallic iron and a quadrupole splitting $\Delta E_q = 2.3$ mm/s and line width $\Gamma = 0.40$ mm/s. These values are typical of high-spin iron(II) porphyrinate complexes.[17]

An overall view of the molecular structure of [Fe(Piv$_2$C$_8$)(1-MeIm) is given in Figure 2. This is a stereoscopic ORTEP2 view contoured at the 50% probability level. Both principal and boundary ellipses are drawn for porphyrin core atoms, strap (or basket-handle) atoms, and axial imidazole atoms; the remaining atoms have only boundary ellipses drawn. The atom labeling scheme used in the tables is given in Figure 3. This figure is a line drawing having the same relative orientation as that of Figure 2. Listings of individual bond distances and angles are given in

Table II. Bond Distances (Å) for [Fe(Piv$_2$C$_8$)(1-MeIm)][a]

atom 1	atom 2	distance	atom 1	atom 2	distance
Fe	N(1)	2.049 (15)	Fe	N(2)	2.095 (14)
Fe	N(3)	2.083 (14)	Fe	N(4)	2.071 (14)
Fe	N(9)	2.134 (21)	N(1)	C(a1)	1.42 (2)
N(1)	C(a2)	1.35 (2)	N(2)	C(a3)	1.35 (2)
N(2)	C(a4)	1.38 (2)	N(3)	C(a5)	1.34 (2)
N(3)	C(a6)	1.37 (2)	N(4)	C(a7)	1.43 (2)
N(4)	C(a8)	1.34 (2)	C(a1)	C(b1)	1.42 (2)
C(a1)	C(m4)	1.38 (2)	C(a2)	C(b2)	1.42 (3)
C(a2)	C(m1)	1.42 (2)	C(a3)	C(b3)	1.50 (2)
C(a3)	C(m1)	1.36 (2)	C(a4)	C(b4)	1.51 (2)
C(a4)	C(m2)	1.34 (2)	C(a5)	C(b5)	1.42 (2)
C(a5)	C(m2)	1.41 (2)	C(a6)	C(b6)	1.41 (2)
C(a6)	C(m3)	1.35 (2)	C(a7)	C(b7)	1.36 (2)
C(a7)	C(m3)	1.43 (3)	C(a8)	C(b8)	1.46 (2)
C(a8)	C(m4)	1.41 (3)	C(b1)	C(b2)	1.38 (2)
C(b3)	C(b4)	1.38 (2)	C(b5)	C(b6)	1.34 (2)
C(b7)	C(b8)	1.42 (3)	C(m1)	C(1)	1.46 (2)
C(m2)	C(7)	1.52 (2)	C(m3)	C(13)	1.58 (2)
C(m4)	C(19)	1.47 (3)	O(1)	C(25)	1.18 (3)
O(2)	C(30)	1.25 (4)	O(3)	C(37)	1.21 (2)
O(4)	C(42)	1.24 (3)	N(5)	C(2)	1.32 (3)
N(5)	C(25)	1.45 (3)	N(6)	C(8)	1.32 (3)
N(6)	C(30)	1.33 (4)	N(7)	C(14)	1.35 (3)
N(7)	C(37)	1.49 (3)	N(8)	C(20)	1.31 (3)
N(8)	C(42)	1.27 (3)	N(9)	C(43)	1.35 (4)
N(9)	C(45)	1.25 (3)	N(10)	C(43)	1.45 (4)
N(10)	C(44)	1.34 (4)	N(10)	C(46)	1.53 (5)
C(1)	C(2)	1.42 (3)	C(1)	C(6)	1.39 (3)
C(2)	C(3)	1.40 (3)	C(3)	C(4)	1.34 (3)
C(4)	C(5)	1.30 (3)	C(5)	C(6)	1.48 (3)
C(7)	C(8)	1.34 (3)	C(7)	C(12)	1.43 (3)
C(8)	C(9)	1.36 (3)	C(9)	C(10)	1.43 (3)
C(10)	C(11)	1.17 (4)	C(11)	C(12)	1.36 (3)
C(13)	C(14)	1.35 (3)	C(13)	C(18)	1.34 (4)
C(14)	C(15)	1.44 (3)	C(15)	C(16)	1.40 (3)
C(16)	C(17)	1.40 (3)	C(17)	C(18)	1.44 (3)
C(19)	C(20)	1.34 (3)	C(19)	C(24)	1.37 (3)
C(20)	C(21)	1.56 (3)	C(21)	C(22)	1.30 (3)
C(22)	C(23)	1.27 (3)	C(23)	C(24)	1.44 (3)
C(25)	C(26)	1.48 (4)	C(26)	C(27)	1.50 (5)
C(26)	C(28)	1.70 (4)	C(26)	C(29)	1.57 (5)
C(30)	C(31)	1.47 (4)	C(31)	C(32)	1.46 (4)
C(32)	C(33)	1.60 (4)	C(33)	C(34)	1.46 (4)
C(34)	C(35)	1.56 (4)	C(35)	C(36)	1.68 (4)
C(36)	C(42)	1.51 (4)	C(37)	C(38)	1.40 (3)
C(38)	C(39)	1.40 (4)	C(38)	C(40)	1.55 (6)
C(38)	C(41)	1.44 (4)	C(44)	C(45)	1.24 (4)

[a] Numbers in parentheses are estimated standard deviations in the least significant digit(s).

(16) Reed, C. A.; Mashiko, T.; Scheidt, W. R.; Spartalian, K.; Lang, G. *J. Am. Chem. Soc.* **1980**, *102*, 2302–2306.
(17) Sams, J. R.; Tsin, T. B. *Porphyrins* **1975**, *IVB*, 425–478.

Table III. Bond Angles (deg) for [Fe(Piv_2C_8)(1-MeIm)][a]

atom 1	atom 2	atom 3	angle	atom 1	atom 2	atom 3	angle
N(1)	Fe	N(2)	88.4 (6)	N(1)	Fe	N(3)	161.7 (7)
N(1)	Fe	N(4)	87.7 (6)	N(1)	Fe	N(9)	99.9 (7)
N(2)	Fe	N(3)	89.0 (5)	N(2)	Fe	N(4)	163.4 (8)
N(2)	Fe	N(9)	103.1 (8)	N(3)	Fe	N(4)	89.8 (6)
N(3)	Fe	N(9)	98.3 (8)	N(4)	Fe	N(9)	93.4 (7)
C(a1)	N(1)	C(a2)	107.9 (16)	C(a3)	N(2)	C(a4)	110.9 (15)
C(a5)	N(3)	C(a6)	108.3 (15)	C(a7)	N(4)	C(a8)	106.7 (17)
N(1)	C(a1)	C(b1)	107.4 (17)	N(1)	C(a1)	C(m4)	127.7 (18)
C(b1)	C(a1)	C(m4)	124.7 (20)	N(1)	C(a2)	C(b2)	108.9 (18)
N(1)	C(a2)	C(m1)	126.1 (18)	C(b2)	C(a2)	C(m1)	124.7 (17)
N(2)	C(a3)	C(b3)	106.2 (16)	N(2)	C(a3)	C(m1)	127.7 (17)
C(b3)	C(a3)	C(m1)	124.6 (15)	N(2)	C(a4)	C(b4)	109.0 (15)
N(2)	C(a4)	C(m2)	126.4 (17)	C(b4)	C(a4)	C(m2)	124.4 (17)
N(3)	C(a5)	C(b5)	108.3 (14)	N(3)	C(a5)	C(m2)	126.1 (15)
C(b5)	C(a5)	C(m2)	125.5 (16)	N(3)	C(a6)	C(b6)	108.4 (17)
N(3)	C(a6)	C(m3)	124.9 (19)	C(b6)	C(a6)	C(m3)	126.7 (18)
N(4)	C(a7)	C(b7)	109.3 (20)	N(4)	C(a7)	C(m3)	122.8 (18)
C(b7)	C(a7)	C(m3)	127.7 (20)	N(4)	C(a8)	C(b8)	110.5 (19)
N(4)	C(a8)	C(m4)	125.7 (20)	C(b8)	C(a8)	C(m4)	123.1 (21)
C(a1)	C(b1)	C(b2)	107.0 (19)	C(a2)	C(b2)	C(b1)	108.2 (18)
C(a3)	C(b3)	C(b4)	110.1 (16)	C(a4)	C(b4)	C(b3)	103.4 (15)
C(a5)	C(b5)	C(b6)	108.1 (17)	C(a6)	C(b6)	C(b5)	107.8 (16)
C(a7)	C(b7)	C(b8)	109.6 (20)	C(a8)	C(b8)	C(b7)	103.7 (20)
C(a2)	C(m1)	C(a3)	124.2 (16)	C(a2)	C(m1)	C(1)	116.5 (17)
C(a3)	C(m1)	C(1)	118.6 (17)	C(a4)	C(m2)	C(a5)	126.3 (17)
C(a4)	C(m2)	C(7)	116.4 (15)	C(a5)	C(m2)	C(7)	117.2 (15)
C(a6)	C(m3)	C(a7)	128.8 (18)	C(a6)	C(m3)	C(13)	118.7 (19)
C(a7)	C(m3)	C(13)	112.2 (17)	C(a1)	C(m4)	C(a8)	122.5 (19)
C(a1)	C(m4)	C(19)	117.6 (18)	C(a8)	C(m4)	C(19)	118.8 (18)
C(2)	N(5)	C(25)	131.5 (21)	C(8)	N(6)	C(30)	132.3 (29)
C(14)	N(7)	C(37)	134.7 (19)	C(20)	N(8)	C(42)	121.6 (25)
C(43)	N(9)	C(45)	112 (3)	C(43)	N(10)	C(44)	109 (3)
C(43)	N(10)	C(46)	117 (3)	C(44)	N(10)	C(46)	134 (4)
C(m1)	C(1)	C(2)	121.4 (25)	C(m1)	C(1)	C(6)	119.4 (24)
C(2)	C(1)	C(6)	118.9 (18)	N(5)	C(2)	C(1)	116.1 (20)
N(5)	C(2)	C(3)	122.2 (22)	C(1)	C(2)	C(3)	121.6 (23)
C(2)	C(3)	C(4)	115.4 (24)	C(3)	C(4)	C(5)	129.4 (26)
C(4)	C(5)	C(6)	116.4 (25)	C(1)	C(6)	C(5)	118.1 (21)
C(m2)	C(7)	C(8)	118.0 (20)	C(m2)	C(7)	C(12)	122.9 (19)
C(8)	C(7)	C(12)	119.0 (20)	N(6)	C(8)	C(7)	116.4 (22)
N(6)	C(8)	C(9)	123.0 (26)	C(7)	C(8)	C(9)	120.3 (25)
C(8)	C(9)	C(10)	118.3 (26)	C(9)	C(10)	C(11)	117.4 (27)
C(10)	C(11)	C(12)	131 (3)	C(7)	C(12)	C(11)	113.5 (23)
C(m3)	C(13)	C(14)	123.0 (27)	C(m3)	C(13)	C(18)	112.1 (25)
C(14)	C(13)	C(18)	124.9 (22)	N(7)	C(14)	C(13)	120.2 (21)
N(7)	C(14)	C(15)	118.1 (22)	C(13)	C(14)	C(15)	121.7 (24)
C(14)	C(15)	C(16)	111.9 (25)	C(15)	C(16)	C(17)	127.8 (23)
C(16)	C(17)	C(18)	115.1 (27)	C(13)	C(18)	C(17)	118.4 (27)
C(m4)	C(19)	C(20)	117.1 (24)	C(m4)	C(19)	C(24)	121.2 (24)
C(20)	C(19)	C(24)	121.7 (25)	N(8)	C(20)	C(19)	125.6 (28)
N(8)	C(20)	C(21)	117.7 (28)	C(19)	C(20)	C(21)	116.3 (27)
C(20)	C(21)	C(22)	115.0 (27)	C(21)	C(22)	C(23)	129.6 (28)
C(22)	C(23)	C(24)	117.0 (25)	C(19)	C(24)	C(23)	120.2 (26)
O(1)	C(25)	N(5)	113 (3)	O(1)	C(25)	C(26)	129 (4)
N(5)	C(25)	C(26)	115.8 (27)	C(25)	C(26)	C(27)	103 (3)
C(25)	C(26)	C(28)	101.3 (27)	C(25)	C(26)	C(29)	116 (3)
C(27)	C(26)	C(28)	112 (3)	C(27)	C(26)	C(29)	123 (3)
C(28)	C(26)	C(29)	100.0 (29)	O(2)	C(30)	N(6)	122 (4)
O(2)	C(30)	C(31)	121 (4)	N(6)	C(30)	C(31)	117 (3)
C(30)	C(31)	C(32)	122 (3)	C(31)	C(32)	C(33)	114.5 (28)
C(32)	C(33)	C(34)	114.7 (28)	C(33)	C(34)	C(35)	103.8 (26)
C(34)	C(35)	C(36)	105.4 (25)	C(35)	C(36)	C(42)	116.9 (28)
O(3)	C(37)	N(7)	110.8 (25)	O(3)	C(37)	C(38)	130.9 (28)
N(7)	C(37)	C(38)	116.8 (23)	C(37)	C(38)	C(39)	118 (3)
C(37)	C(38)	C(40)	105 (3)	C(37)	C(38)	C(41)	104.7 (25)
C(39)	C(38)	C(40)	106 (3)	C(39)	C(38)	C(41)	111.9 (29)
C(40)	C(38)	C(41)	112 (4)	O(4)	C(42)	N(8)	122 (3)
O(4)	C(42)	C(36)	118 (3)	N(8)	C(42)	C(36)	115.4 (29)
N(9)	C(43)	N(10)	98.3 (26)	N(10)	C(44)	C(45)	105 (4)
N(9)	C(45)	C(44)	114 (3)				

[a] Numbers in parentheses are estimated standard deviations in the least significant digit(s).

Tables II and III, respectively. Within the relatively large, but understandable, uncertainties of individual bond distances and angles of the core, bond parameters of the porphyrin ligand are normal.

The synthetic strategy, i.e., the formation of a porphyrin ligand with one highly hindered face that will yield five-coordinate species with unhindered axial ligands, is nicely illustrated by the crystal structure. Important aspects can be seen in Figure 4, a space-

Table IV. Summary of Parameters for Five-Coordinate High-Spin Iron(II) and Manganese(II) Porphyrinates[a]

compd	Fe–N_p	Fe–Ax	Ct···N	Fe displacement 4N	Fe displacement 24-atom	ref
[Fe(Piv_2C_8)(1-MeIm)]	2.075 (20)	2.134 (21)[b]	2.051	0.31	0.34	this work
[Fe(TPivP)(2-MeHIm)]	2.072 (6)	2.095 (6)[b]	2.033	0.40	0.43	10
[Fe(TPP)(2-MeHIm)]	2.086 (8)	2.161 (5)[b]	2.044	0.42	0.55	8
[Fe(TPivP)Cl]$^-$	2.108 (15)	2.301 (2)[c]	2.040	0.53	0.59	24b
[Fe(TPivP)(SC_6HF_4)]$^-$	2.076 (20)	2.370 (3)[d]	2.033	0.42	–[e]	24b
[Fe(TPP)(SC_2H_5)]$^-$	2.096 (4)	2.360 (2)[d]	2.030	0.52	0.62	24a
[Fe(TPivP)(O_2CCH_3)]$^-$	2.107 (2)	2.034 (3)[f]	2.033	0.55	0.64	24c
[Fe(TPivP)(OC_6H_5)]$^-$	2.114 (2)	1.937(4)[f]	2.037	0.56	0.62	24c
[Mn(TPP)(1-MeIm)]	2.128 (2)	2.192 (2)[b]	2.065	0.51	0.56	26

[a] All values in angstroms. [b] Imidazole. [c] Chloride. [d] Thiolate. [e] Not reported. [f] Anionic oxygen donor.

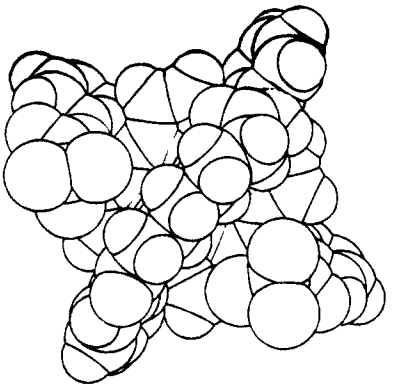

Figure 4. Space-filling model (SHAKAL) of [Fe(Piv_2C_8)(1-MeIm)] viewed perpendicular to the highly hindered face. Only the hydrogen atoms included in the crystallographic refinement are displayed; thus the hydrogen atoms on the *tert*-butyl pickets are not illustrated.

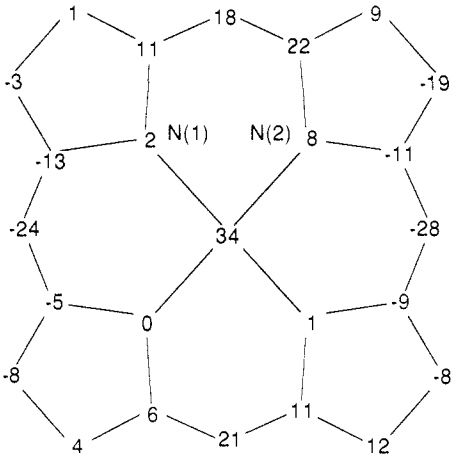

Figure 5. Formal diagram of the porphinato core in [Fe(Piv_2C_8)(1-MeIm)] displaying the perpendicular displacement of each atom (in units of 0.01 Å) from the mean plane of the 24-atom core. To assist in orienting the viewer, the labels for two porphinato nitrogen atoms are shown.

filling drawing of [Fe(Piv_2C_8)(1-MeIm)]. The key element of the ligand design is clearly evident: the bis(amido)alkane strap blocks access to iron and the two trans pivaloyl pickets prevent lateral movement of the strap that might allow access of an axial imidazole ligand to the face. The fact that a strap alone is only partially effective in protecting an iron(II) porphyrinate face has been noted previously.[18] The strap was intended to be of sufficient length to mimimize effects on the core conformation; it is known that the constraints of a short strap can cause marked core deformations.[19] Nevertheless, it is likely that the S_4 ruffling of the core (vide infra) is caused at least in part by linking the two trans phenyl rings via the –NH–C(O)–$(CH_2)_6$–C(O)–NH– strap. Figure 5 presents a formal diagram of the porphinato core in [Fe(Piv_2C_8)(1-MeIm)] that displays the perpendicular displacements (in units of 0.01 Å) of the core atoms from the 24-atom mean plane. As clearly seen from this diagram, the core has a pattern of displacements approximately consistent with S_4 ruffling; however, the deviations from that idealized symmetry are quite large. Atoms with positive displacement values are on the axial imidazole ligand side of the porphinato plane. The two *meso*-carbon atoms along the horizontal axis of the diagram are joined by the strap and are displaced toward the hindered side of the porphyrin. The constraint of the strap is not simply one of strap length but also one of the conformation along the chain. We note that one of the two amido groups of the strap is not coplanar with its attached phenyl as might be expected under unconstrained conditions. It can also be seen in Figure 2 that the strap connected phenyl groups "droop" to the hindered face side of the porphyrin ligand. The chain link does not otherwise appear to affect the orientation of the peripheral phenyl rings in a substantial manner: the dihedral angles between these two phenyl rings and the mean plane of the core are 68.5 and 74.6°. The other two phenyl groups form dihedral angles of 74.0 and 81.2°. All four values are within the normal range. These structural features are readily seen in Figure 2.

Before comparing 1-methylimidazole-ligated iron(II) with 2-methylimidazole-ligated iron(II) we must address the question of whether the ruffled core conformation leads to significant effects on the coordination group bond parameters of [Fe(Piv_2C_8)(1-MeIm)]. It should be noted that S_4 ruffling is known to be an accommodating geometry for the coordination of metal ions requiring *short* metal–nitrogen bonds and indeed ruffling is a major geometric mechanism for bond shortening in metalloporphyrins.[20] However, this type of ruffling is not a core conformation typically observed in metalloporphyrin derivatives with large metal ions. Indeed, we have recently surveyed the core conformations of all tetraarylporphinato derivatives in the literature.[21] There is only one example of a metalloporphyrin derivative having both a relatively large metal ion and also a significantly S_4-ruffled core, the "tailed" porphyrin derivative [Zn(TPP-C_3Py)].[22] In this complex, the observed Zn–N_p bonds are shortened by no more than 0.01 Å as a consequence of the core ruffling.[23] Since M–N_p bonds in five-coordinate zinc(II) porphyrinates are almost as long as those expected for high-spin iron(II), these zinc observations set something of a limit on the effects of the ruffled core in [Fe(Piv_2C_8)(1-MeIm)] on the Fe–N_p bond distances.

The average Fe–N_p bond distance in [Fe(Piv_2C_8)(1-MeIm)] is 2.075 (20) Å, a value just at the low end of previous observations[8,10,24] for iron(II) porphyrinates. Pertinent stereochemical

(18) Momenteau, M.; Mispelter, J.; Loock, B., Lhoste, J.-M. *J. Chem. Soc., Perkin Trans. 2* **1985**, 61–70.
(19) Simonis, U.; Walker, F. A.; Lee, P. L.; Hanquet, B. J.; Meyerhoff, D. J.; Scheidt, W. R. *J. Am. Chem. Soc.* **1987**, *109*, 2659–2668. Wijeserkera, T. P.; Paine, J. B.; Dolphin, D.; Einstein, F. W. B.; Jones, T. *J. Am. Chem. Soc.* **1983**, *105*, 6747–6749.
(20) Hoard, J. L. *Ann. N.Y. Acad. Sci.* **1973**, *206*, 18–31. Collins, D. M.; Scheidt, W. R.; Hoard, J. L. *J. Am. Chem. Soc.* **1972**, *94*, 6689–6696.
(21) Scheidt, W. R.; Lee, Y. J. *Struct. Bonding* **1987**, *64*, 1–70.
(22) Bobrick, M. A.; Walker, F. A. *Inorg. Chem.* **1980**, *19*, 3383–3390.
(23) The average Zn–N bond distance observed in [Zn(TPP-C_3Py)] is 2.059 Å compared to an average value of 2.069 Å for four other pyridine-ligated zinc porphyrinates.

parameters for the structurally characterized five-coordinate high-spin iron(II) porphyrinates are listed in Table IV. As can be seen from the table, there is substantial structural variation between these derivatives. In our 1981 review,[25] we emphasized that the stereochemical parameters of iron porphyrinates could be categorized by spin state, coordination number, and oxidation state; the simple definition of these descriptors leads to the prediction of the complex's structure within narrow limits. Subsequent structural work has made it evident that the overall charge on the complex is also a significant factor: a negative charge leads to increased Fe–N_p bond distances. This charge effect is also clearly evident in the entries of Table IV; the last five iron entries are those for anionic complexes. It is to be noted that, even after allowing for the probable charge effect on coordination parameters, five-coordinate high-spin iron(II) porphyrinate species show somewhat larger variation than those of otherwise analogous iron(III) species.

The iron(II) atom is displaced 0.31 Å from the mean plane of the four nitrogen atoms and 0.34 Å from the best least-squares plane of the 24-atom core. These atomic displacements are the smallest yet observed for a high-spin iron(II) complex. The metal atom displacements are interrelated with two other geometrical features—core doming and radial expansion of the core (hole size). Core doming has frequently been found in five-coordinate iron(II) porphyrinates but not iron(III) derivatives. Porphinato core doming is conveniently measured by the difference in displacement of the metal ion from the mean plane of the four nitrogen atoms and the 24-atom core. As can be seen from Table IV, several of the iron(II) complexes display a doming of ~0.1 Å or more. Five-coordinate high-spin iron(III) complexes, on the other hand, typically display doming of <0.05 Å. The precise reasons for the occurrence of doming remain unclear although the effect is seen for a number of other metalloporphyrin species having large metal ions. Indeed, core doming is only observed in species with large metal ions, and the larger the metal ion the more likely doming will be observed. In these cases, the pyrrole nitrogen atoms "follow" the metal atom out of plane leading to doming. One interesting example where doming is not observed is also listed in Table IV, high-spin [Mn(TPP)(1-MeIm)].[26] This complex has a large metal ion and a single unhindered imidazole ligand.

Large metal atom displacements are expected for five-coordinate porphinato derivatives having long M–N_p bonds. This results from a general constraint of porphinato cores that limits the radial expansion of the central hole. This expansion is conveniently measured by the radius of the central hole, the Ct···N distance, where Ct is the center of the porphyrin macrocycle. As can be seen from Table IV, the metal atom displacement and the M–N_p bond length are interrelated with the radius of the central hole. Once the metal atom displacement and the Fe–N_p bond distance are specified the value of Ct···N is fixed. Its relatively large value in [Fe(Piv_2C_8)(1-MeIm)] (2.051 Å) is unexpected on two counts. First, the effect of the S_4 core ruffling is usually to decrease rather than increase the radius of the central hole.[20] Second, as pointed out by Hoard[27] many years ago, there must exist a hole radius corresponding to least strain in the macrocycle. The value suggested, 2.01 Å, is smaller than that observed (Table IV) for any iron(II) complex. The wide variation in metal atom displacement, M–N_p, and Ct···N distances for the iron(II) porphyrinates apparently reflects the interrelated subtlety in achieving the most energetically favorable geometry for the complex. A yet unresolved problem for iron(II) porphyrinates is understanding this variation; other metalloporphyrin species appear to find a single minimum for the structural parameters of a given class.[28]

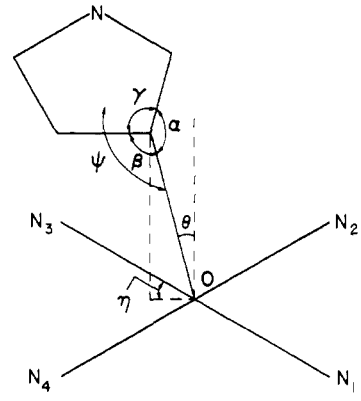

Figure 6. Diagram illustrating the geometric parameters used to describe the coordination of imidazoles in metalloporphyrin species.

The imidazole ligand plane forms a dihedral angle of 34.1° with the coordinate plane defined by Fe, N(9), and N(2). This angle, commony called ϕ, is much larger than any previously observed[29] in five-coordinate metalloporphyrins wherein the average ϕ value is 10.4° and the previous largest value is 23°. Curiously, the imidazole is oriented so that its plane is more nearly above the *meso*-carbon atoms carrying the picket-substituted phenyl rings. Thus, the imidazole ring is close to being directly above the *meso*-carbon atoms that are displaced to the imidazole side of the porphyrin plane rather than in the sterically more favorable orientation where the ring would nestle in the hollows of the S_4-ruffled core. The sterically expected orientation is observed in the low-spin six-coordinate complex with two sterically hindered 2-methylimidazole ligands;[30] the two methyl groups each nestle in such hollows. It would thus appear that there is no intramolecular steric reason for the observed imidazole orientation in [Fe(Piv_2C_8)(1-MeIm)].

The axial bond distance, Fe–N(Im), is 2.134 (21) Å. This is between the values observed for the two iron(II) species (Table IV) bearing a 2-methylimidazole ligand. However, the 2.095-Å value reported for [Fe(TPivP)(2-MeHIm)][10] is likely to be slightly underestimated owing to the description of the imidazole ligand used in the rigid-group refinement.[31] The differences in the axial Fe–N(Im) bond distances appear to be little affected by the hindering methyl substituent. A 0.06-Å difference has been found in two cobalt(II) porphyrinates bearing respectively unhindered[32] and hindered[33] imidazole ligands, but because the steric demands of the axial ligand are accentuated in cobalt(II) by the substantially smaller displacements of the metal atom we do not expect as large a difference with iron(II). Thus, of the coordination parameters considered in Table IV, we conclude that only the somewhat smaller displacement of the iron atom in the present structure is a result of the unhindered vs hindered ligand variation.

In this final section, we turn to a comparison of the geometry of the axial ligand interaction with the metal ion in fiv-coordinate imidazole-ligated metalloporphyrin derivatives. Are any of the

(24) (a) Caron, C.; Mitschler, A.; Riviere, G.; Schappacher, M.; Weiss, R. *J. Am. Chem. Soc.* **1979**, *101*, 7401–7402. (b) Schappacher, M.; Ricard, L.; Weiss, R.; Montiel-Montoya R.; Gonser, U.; Bill, E.; Trautwein, A. *Inorg. Chim. Acta* **1983**, *78*, L9–L12. (c) Nasri, H.; Fischer, J.; Weiss, R.; Bill, E.; Trautwein, A. *J. Am. Chem. Soc.* **1987**, *109*, 2549–2550.

(25) Scheidt, W. R.; Reed, C. A. *Chem. Rev.* **1981**, *81*, 543–555.

(26) Kirner, J. F.; Reed, C. A.; Scheidt, W. R. *J. Am. Chem. Soc.* **1977**, *99*, 2557–2563.

(27) Collins, D. M.; Hoard, J. L. *J. Am. Chem. Soc.* **1970**, *92*, 3761–3771.

(28) For five-coordinate species with an adequate number of structures, in addition to the already mentioned iron(III) species, manganese(III), cobalt(II), and zinc(II) all show a narrow range for their respective coordination parameters.

(29) Scheidt, W. R.; Chipman, D. M. *J. Am. Chem. Soc.* **1986**, *108*, 1163–1167.

(30) Scheidt, W. R.; Kirner, J. F.; Hoard, J. L.; Reed, C. A. *J. Am. Chem. Soc.* **1987**, *109*, 1963–1968.

(31) The geometry used in defining the rigid group has a value for the internal angle subtended at the coordinating nitrogen that is unrealistically small. Since the rigid group refinement will essentially position the ring at the center of gravity, this small angle has the effect of placing the nitrogen atom too close to the iron. Another choice, in disagreement with observation, is that of essentially equivalent exo angles at the 2-position. This will also effect the position of the imidazole ring.

(32) Scheidt, W. R. *J. Am. Chem. Soc.* **1974**, *96*, 90–94. The Co–N(Im) distance is 2.157 (3) Å and the cobalt(II) displacement is 0.14 Å from the 24-atom plane.

(33) Dwyer, P. N.; Madura, P.; Scheidt, W. R. *J. Am. Chem. Soc.* **1974**, *96*, 4815–4819. The Co–N(Im) distance is 2.216 (2) Å and the cobalt(II) displacement is 0.18 Å from the 24-atom plane.

Table V. Imidazole Coordination in Five-Coordinate Metalloporphyrins.[a]

complex	M–N[b]	D.A.[c,d]	α[c]	β[c]	γ[c]	η[c]	θ[c]	ψ[c]	ref
[Mn(TPP)(1-MeIm)]	2.192 (2)	82.8	130.4	125.2	104.4	29.5	8.0	180.4	26
[Fe(OEP)(2-MeHIm)]$^+$	2.068 (4)	88.0	131.7	122.1	106.2	89.7	4.0	178.4	35
[Fe(Piv_2C_8)(1-MeIm)]	2.134 (21)	81.3	126.5	120.4	112.0	80.8	5.0	174.3	this work
[Fe(TPivP)(2-MeHIm)]	2.095 (6)	89.8	132.1	126.3	101.6[e]	15.8	9.5	179.1	10
[Fe(TPP)(2-MeHIm)]	2.161 (5)	88.1	131.4	122.6	106.1[e]	87.6	10.2	176.6	8
[Co(TPP)(1-MeIm)]	2.157 (3)	82.8	127.8	126.4	105.6	54.3	4.5	176.1	32
[Co(OEP)(1-MeIm)]	2.15 (1)	87.8	126.8	126.4	106.9	63.7	1.0	178.9	36
[Co(TPP)(1,2-DiMeIm)]	2.216 (2)	89.1	132.6	122.5	104.9	6.8	6.3	177.6	33
[Zn(OEP)(1-MeIm)]	2.106 (4)	86.8	127.3	127.8	104.8	55.7	1.5	178.4	37

[a] All angles denoted by Greek letters are defined in Figure 6. [b] Value in Å. [c] Value in degrees. [d] D.A. is the dihedral angle between the ligand plane and the porphinato mean plane. [e] Value fixed in rigid-group refinement.

Table VI. Imidazole Coordination in Six-Coordinate Metalloporphyrins[a]

complex	M–N[b]	D.A.[c,d]	α[c]	β[c]	γ[c]	η[c]	θ[c]	φ[c]	ref
[Mg(TPP)(1-MeIm)$_2$]	2.297 (8)	87.0	129.6	126.9	103.5	85.8	1.6	178.6	38
[Mn(TPP)(Im$^-$)]$_n$[e]	2.186 (5)	86.3	134.4	123.6	101.7	20.8	1.3	178.3	39
—[e,f]	2.280 (4)	80.3	133.0	124.3	102.4	37.7	3.6	175.6	
[Mn(TPP)(1-MeIm)$_2$]$^+$[e]	2.308 (3)	84.2	128.7	127.8	103.4	72.1	3.1	178.4	40
[Fe(TPP)(HIm)$_2$]Cl	1.991 (5)	84.0	125.6	127.7	106.7	63.5	2.2	177.7	41
	1.957 (4)	85.1	126.1	127.7	106.1	173.5	178.3	175.4	
[Fe(TPP)(HIm)$_2$]Cl·H_2O[e]	1.977 (3)	86.4	127.3	127.8	104.8	73.3	0.6	182.0	42
—[e,f]	1.966 (5)	87.0	125.7	128.8	105.4	60.0	0.8	178.2	
[Fe(Proto IX)(1-MeIm)$_2$]	1.988 (5)	88.3	128.1	127.0	104.9	60.8	1.4	181.0	43
	1.966 (5)	89.3	128.8	126.5	104.7	198.2	181.4	180.8	
[Fe(TPP)(2-MeHIm)$_2$]$^+$	2.015 (4)	77.9	133.2	120.6	105.6	70.5	4.3	171.9	29
	2.010 (4)	85.7	132.5	120.5	106.7	315.5	182.6	176.6	
[Fe(OEP)(2-MeHIm)$_2$]$^+$[e]	2.275 (1)	86.2	134.2	120.8	105.0	45.8	3.3	178.3	44
[Fe(TPP)(BzHIm)$_2$]$^+$[e]	2.216 (5)	88.1[g]	134.5	121.8	103.8	80.3	3.1	178.2	45
[Fe(TPP)(4-MeIm$^-$)$_2$]$^-$	1.928 (12)	88.2	130.9	127.9	101.2	78.5	1.0	182.3	46
	1.958 (12)	88.7	129.7	125.2	105.1	222.9	181.2	178.4	
[Fe(TPP)(1-MeIm)$_2$][e]	2.014 (5)	88.0	128.2	128.3	103.6	39.2	1.1	180.2	40
[Fe(TPP)(NO)(1-MeIm)]	2.180 (4)	82.5	130.5	126.6	102.6	45.2	2.1	175.6	47
[Fe(TPP-C_5Im)(THT)]	2.002 (5)	85.1	130.0	127.8	102.1	10.0	0.6	176.2	48
[Fe(TPivP)(2-MeHIm)(O_2)]	2.107 (4)	89.7	135.0	123.3	101.6[h]	75.4	7.2	178.8	10
[Fe(TPivP)(1-MeIm)(O_2)]	2.07 (2)	90.0[i]	124.0[i]	124.0[i]	112.0[i]	0.0[i]	0.0[i]	180.0[i]	49
[Ni(TMPyP)(HIm)$_2$][e]	2.160 (4)	83.0	128.5	126.0	105.5	64.6	2.8	178.1	50

[a] All angles denoted by Greek letters are defined in Figure 6. [b] Value in Å. [c] Value in degrees. [d] D.A. is the dihedral angle between the ligand plane and the porphinato mean plan. [e] Complex has required inversion symmetry. [f] Independent molecule. [g] Four nitrogen plane. [h] Value fixed in rigid-group refinement. [i] Value fixed by required twofold symmetry.

geometrical parameters involving the imidazole ligand materially affected y the use of a nonhindered imidazole ligand relative to a sterically demanding one? This comparison was motivated by the observation that the imidazole plane in [Fe(Piv_2C_8)(1-MeIm)] is rather "tilted" and makes a dihedral angle of 81.3° with the mean plane of the core. It has long been recognized[34] that imidazole and substituted imidazole ligands frequently coordinate to metal ions in a rather nonidealized fashion. We have carried out a systematic survey of the coordination geometry of imidazole ligands in metalloporphyrin complexes to determine the extent of the "nonideality". The calculations can be understood in terms of a number of angles that are defined in Figure 6. The metal atom of the complex is always taken as the origin of the coordinate system. Three particular geometric features merit mention. First is the deviation of the M–N(Im) vector from normality to the porphyrin plane: the two components, θ, the "tipping" angle, and η, the projection of the vector onto the porphinato plane (the x,y coordinate system defined in terms of the porphinato nitrogen atoms), are of particular interest. Second is the tilting of the imidazole from the M–N(Im) vector, defined in terms of the differences in the angles α and β. A significantly larger α angle serves to relieve strain induced by a substituent at the 2-position of the imidazole ligand. However, it should be noted that even when there is no 2-substituent, the angle α is frequently the much larger of the two. The third geometric parameter is the tilting of the imidazole ring plane from the M–N(Im) vector denoted by ψ. These values are tabulated in Table V for structurally characterized five-coordinate species. As can be seen from this table, the values for [Fe(Piv_2C_8)(1-MeIm)] are not exceptional. A number of derivatives show significant deviations from ideality. Analogous calculations for five-coordinate pyridine-ligated species show much smaller variations in geometry. For completeness in describing the imidazole coordination geometry in metalloporphyrins, we have also calculated the geometric descriptors for six-coordinate derivatives. Values for both mixed axial ligand and bis(imidazole) complexes are given in Table VI. The values are not remarkable in comparison to those reported for the five-coordinate species given in Table V.[35-50]

(34) Freeman, H. C. *Adv. Protein Chem.* **1967**, *22*, 305–308.
(35) Scheidt, W. R.; Geiger, D. K.; Lee, Y. J.; Reed, C. A.; Lang, G. *J. Am. Chem. Soc.* **1985**, *107*, 5693–5699.
(36) Little, R. G.; Ibers, J. A. *J. Am. Chem. Soc.* **1974**, *96*, 4452–4463.
(37) Brennan, T. D.; Scheidt, W. R. *Acta Crystallogr. Sect. C*, in press.
(38) McKee, V.; Ong, C. C.; Rodley, G. A. *Inorg. Chem.* **1984**, *23*, 4242–4248.
(39) Landrum, J. T.; Hatano, K.; Scheidt, W. R.; Reed, C. A. *J. Am. Chem. Soc.* **1980**, *102*, 6729–6735.
(40) Steffen, W. L.; Chun, H. K.; Hoard, J. L.; Reed, C. A. *Abstracts of Papers*; 175th National Meeting of the American Chemical Society; Anaheim CA March 13–17, 1978; American Chemical Society: Washington, D.C., 1978; INOR 15.
(41) Collins, D. M.; Countryman, R.; Hoard, J. L. *J. Am. Chem. Soc.* **1972**, *94*, 2066–2072.
(42) Scheidt, W. R.; Osvath, S. R.; Lee, Y. J. *J. Am. Chem. Soc.* **1987**, *109*, 1958–1963.
(43) Little, R. G.; Dymock, K. R.; Ibers, J. A. *J. Am. Chem. Soc.* **1975**, *97*, 4532–4539.
(44) Geiger, D. K.; Lee, Y. J.; Scheidt, W. R. *J. Am. Chem. Soc.* **1984**, *106*, 6339–6343.
(45) Levan, K. R.; Strouse, C. E. *Abstracts of Papers*; American Crystallographic Association Summer Meeting, Snowmass, CO, Aug 1–5, 1983; Abstract H1.
(46) Quinn, R.; Strouse, C. E.; Valentine, J. S. *Inorg. Chem.* **1983**, *22*, 3934–3940.
(47) Piciulo, P. L.; Scheidt, W. R. *J. Am. Chem. Soc.* **1976**, *98*, 1913–1919.

In summary, the characterization of a five-coordinate iron(II) complex bearing a sterically unhindered axial imidazole ligand has been made possible by the synthesis of a porphyrin having one severely sterically hindered face. The X-ray structure reveals that some subtle stereochemical effects are introduced by the face-hindering superstructure, but even so, the molecule must fairly closely approach the intrinsic unconstrained coordination geometry of a high-spin iron(II) imidazole-ligated heme. A structural comparison with complexes having a sterically hindered 2-methyl imidazole axial ligand reveals a relatively small but apparently significant stereochemical influence of the 2-methyl group. A slightly larger out-of-plane iron atom displacement (≈0.1 Å) and a slightly greater tilting of the imidazole ring (≈5° in angles θ and α of Figure 6) are the structurally identifiable effects of introducing a 2-methyl substituent. In a general sense, the present work endorses the 2-methylimidazole steric hindrance paradigm as a way of achieving relatively unconstrained five-coordination with iron(II) porphyrinates. But in detail, it suggests that in such complexes, the out-of-plane iron displacement and imidazole tilt will be greater in a fully relaxed structure. Perutz[51] has pointed out that the difference in out-of-plane displacement between the two types of model complexes parallels that between human T-state deoxyhemoglobin (α, 0.58 (3); β, 0.50 (3) Å)[52] and a recent novel structure of horse R-state deoxyhemoglobin (α, 0.41; β, 0.45 Å).[51] Thus, at least with respect to the out-of-plane criterion, it appears that the 2-methylimidazole complexes are better structural models of T-state deoxyhemoglobin while the 1-methylimidazole complex is a better model for R-state deoxyhemoglobin. Iron atom displacement and imidazole tilting are key components of mechanisms of cooperative deoxygen binding.[4] That the iron atoms in hemoglobin seem to be slightly further away from their heme planes (rather than closer) compared to an unconstrained model is consistent with the idea of a tethered imidazole that cannot move toward the plane to its optimal relaxed position until the T → R state change has occurred. Curiously, deoxymyoglobin[53] has an out-of-plane iron atom displacement (0.45 Å) that is closer to that of the 2-methylimidazole model than the 1-methylimidazole model. Thus, in spite of its high oxygen affinity, it appears that deoxymyoglobin may also be in a somewhat constrained state.

The protein result that remains somewhat puzzling and, if not artifactual, a great synthetic model challenge is the extremely small iron out-of-plane displacement and reverse doming ($Fe\cdots Ct_N > Fe\cdots Ct$) reported for deoxyerythrocruorin.[54] The possible influence of a distant water molecule in the sixth coordination site has been discussed[25] and more fundamental reservations have been expressed about the resolution limits of protein X-ray crystal structure determinations.[55,56] Nevertheless, as the art of derivatizing porphyrins with elaborate superstructures continues to become more sophisticated,[12,57] it may be interesting to see if constrained porphyrins can enforce unexpected coordination parameters upon high-spin iron(II) porphyrin complexes. Furthermore, since high-spin iron(II) porphyrinates stereochemistry is turning out to be relatively flexible with respect to out-of-plane displacement and imidazole tilting, it will be worthwhile to expand the data base of unconstrained models represented by the single example of the present work. Such studies will be a valuable complement to the improving accuracy of hemoprotein crystallography.

Acknowledgment. We are grateful to Ben Shaevitz and Prof. George Lang for Mössbauer measurements. This work was supported at the University of Southern California by the National Institutes of Health (GM-23851) and at the University of Notre Dame by the National Institutes of Health (GM-38401). We also thank Dr. M. F. Perutz for a preprint of ref 51.

Supplementary Material Available: Anisotropic temperature factor for the iron atom (Table IS), fixed hydrogen atom positions (Table IIS), and rigid group and derived atomic coordinates for the toluene solvate molecule (Table IIIS) (3 pages); tables of observed and calculated structure amplitudes (×10) for [Fe(Piv_2C_8)(1-MeIm)] (8 pages). Ordering information is given on any current masthead page.

(48) Mashiko, T.; Reed, C. A.; Kastner, M. E.; Haller, K. J.; Scheidt, W. R. *J. Am. Chem. Soc.* **1981**, *103*, 5758–5767.
(49) Jameson, G. B.; Rodley, G. A.; Robinson, W. T. Gagne, R. R.; Reed, C. A. Collman, J. P. *Inorg. Chem.* **1978**, *17*, 850–857.
(50) Kirner, J. F.; Garofalo, J., Jr.; Scheidt, W. R. *Inorg. Nucl. Chem. Lett.* **1975**, *11*, 107–112.
(51) Perutz, M. F.; Fermi, G.; Luisa, B.; Shaanan, B.; Liddington, R. *Acc. Chem. Res.* **1987**, *20*, 309–321.
(52) Fermi, G.; Perutz, M. F.; Shaanan, B.; Fourme, R. *J. Mol. Biol.* **1984**, *175*, 159–174.
(53) Takano, T. J. *Mol. Biol.* **1977**, *110*, 569–584.
(54) Steigemann, W.; Weber, E. *J. Mol. Biol.* **1979**, *127*, 309–328.
(55) Parak, F.; Frolov, E. N.; Mossbauer, R. L.; Goldanskii, V. I. *J. Mol. Biol.* **1981**, *145*, 825–833.
(56) A reviewer asks us to note that at least some of the unusual features in the coordination geometry of the heme in the erythrocruorin structure may result from deficiencies in the structural models used in the refinements, for example, the use of a too rigid hydrogen bond between the oxygen ligand and a pocket water molecule.
(57) Larsen, N. G.; Boyd, P. D. W.; Rodgers, S. J.; Wuenschell, G. E.; Koch, C. A.; Rasmussen, S. Tate, J. R.; Erler, B. S.; Reed, C. A. *J. Am. Chem. Soc.* **1986**, *108*, 6950–6960.